MATHEMATICAL MODELING AND SIMULATION OF COMPLEX PHENOMENA IN RAREFIED GASES

Vladimir V. Riabov
Rivier University
420 S. Main Street ▪ Nashua, NH 03060-5086, USA
E-mail: vriabov@rivier.edu

Gas flows near simple-shape bodies (plates, wedges, disks, cylinders, and torus) are studied using the direct simulation Monte-Carlo technique and available software tools. Strong influences of rarefaction and geometrical factors on lift and drag are found.

1. Introduction

Modern aerospace projects require applications of modeling skills and knowledge from various disciplines including physics, chemistry, numerical simulations, etc. In many cases, the "traditional" approaches of solving "classical" differential equations (e.g., the Navier-Stokes equations that describe properties of continuum media) do not work at all. The studies of the probe flights under the rarefied-gas atmospheric conditions require the development of alternative methods of mathematical modeling and simulation that lead to understanding complex phenomena that took place in the media.

Stimulated by planetary exploration programs [1], numerical and experimental studies [1-8] of aerodynamics of simple-shape bodies have provided valuable information related to physics of rarefied-gas flows about spacecraft elements, testing devices, and in micro-channels. Numerous results were found in the cases of plates, wedges, cones, spheres, and cylinders [4-15, 29].

In the present paper, hypersonic rarefied-gas flows about a plate, wedge, disk, two side-by-side cylinders and plates, torus, and spinning cylinder are studied. The role of rare-faction parameter (Knudsen number [2]), specific heat ratio, spinning rates, surface temperature, and geometrical factors is investigated. The DSMC method [2] and DS2G code [14] are used as a numerical technique for simulating low-density gas flows. Molecular collisions in air, nitrogen, carbon dioxide, helium, and argon are modeled using the variable hard sphere model [2]. The gas-surface interactions are assumed to be fully diffusive with full moment and energy accommodation. The validation [9] was tested in comparing numerical results with experimental data [6-8].

2. DSMC Method

The direct simulation Monte Carlo (DSMC) method (described in detail in the Graeme A. Bird's book [2]) and the two-dimensional DS2G code [14] have been used in this study as a numerical simulation technique for low-density hypersonic gas flows. The DSMC method is a computer-simulating technique for the modeling of real-gas effects by a

sample of randomly-selected molecules (thousands or even millions). The position coordinates and velocity components of these molecules are stored in the computer memory and are modified with time as the molecules are concurrently followed through representative collisions and boundary interactions in the simulated physical space [2, 14]. Intermolecular collisions in dilute gases are overwhelmingly likely to be binary collisions involving just two molecules. Given the physical properties of the molecules and the orientation of the trajectories, the post-collision velocities are determined from the equations of linear momentum and energy that must be conserved in the collision (see [2], pp.30-41 for detail).

This direct simulation of the physical processes [2] contrasts with the “traditional” approach of computational fluid dynamics (CFD), which is based on obtaining numerical solutions of the fundamental mathematical equations and proper boundary conditions that model the processes [22]. In the cases of rarefied gas flows, when the gas density is sufficiently low, the direct physical simulation becomes a valuable simulating approach without any recourse to the conventional mathematical models of the flow. Under these conditions, the DSMC method becomes a unique adequate tool, because the full set of the Navier-Stokes equations [7, 22, 23] (or their modifications, e.g., thin-viscous-shock-layer equations [24]) does not provide a valid model for rarefied gases, and conventional CFD methods are unable to handle the large number of independent variables that are involved in applications of the Boltzmann equation [2, 25] to realistic multi-dimensional problems [2]. It has been shown [26] that the Boltzmann equation can be derived through physical reasoning, which is very close to that behind the DSMC procedures, and the two are entirely consistent. For example, the assumptions of molecular chaos and a dilute gas are required by both the Boltzmann formulation and the DSMC method. The major difference between them is the DSMC method does not depend on the existence of inverse collisions [2, 26].

The Knudsen number, which is the ratio of the mean free path to a typical dimension of the flowfield (e.g., a cylinder diameter, a plate length, etc.), characterizes the degree of rarefaction of a gas flow. The Navier-Stokes equations [22] are valid when the Knudsen number is very small in comparison with unity [2, 7]. The opposite limit (as the Knudsen number tends to infinity) is the collisionless or free-molecule flow limit [3], in which intermolecular collisions may be neglected. The flow regime between free-molecule and the limit of validity of the Navier-Stokes equations is generally referred to as the transition flow regime (studied in this paper). A Knudsen number of 0.1 has traditionally been quoted as the boundary between the continuum and transition regimes [2], but the characteristic dimension of complex flow fields may be specified in many different ways and the use of an "overall Knudsen number" may be misleading [14].

The conservation equations of gas dynamics are valid for all flow regimes, but the Navier-Stokes equations depend also on postulates of the Chapman-Enskog theory [25] for the shear stresses, heat fluxes and diffusion velocities as linear functions of the velocity, temperature and concentration gradients. The Chapman-Enskog theory assumes that the velocity distribution is a small perturbation of the equilibrium (or Maxwellian)

distribution. The formulation of the Chapman-Enskog distribution incorporates "local Knudsen numbers" [2, 25] which are the ratios of the local mean free paths to the scale lengths of the velocity and temperature gradients. It has been found that errors become significant when these local Knudsen numbers exceed 0.1 and the continuum theory is hardly useable when they exceed 0.2 [2]. Although it was shown many years ago [2, 25] that the Chapman-Enskog expansion for the distribution function is not uniformly valid, attempts are still being made to extend the range of validity of the Navier-Stokes equations to lower densities (e.g., see [7]).

In addition, some physical effects, such as thermal and pressure diffusion, become more prominent at low densities and these are not generally included in the Navier-Stokes formulations [2]. Once the density becomes sufficiently low, the application of the DSMC method becomes computationally more feasible for the following reasons [14]:

- The calculation is always unsteady with physical time as one of the principal variables in the simulation. A steady flow is obtained as the large time state of the unsteady flow. The method does not require an initial approximation to the flow field and there is no iterative procedure for convergence to the final solution. (In the case of a time averaged steady flow or an ensemble averaged unsteady flow, there is a gradual decline in the statistical scatter as the sample increases [2]).
- Additional effects, such as non-equilibrium chemistry, may be included simply by adding to the complexity of the molecular model [2, 27] and the fact that these may change the basic nature of the continuum equations is of no consequence.
- Finally (and importantly), there are no numerical instabilities.

Another key computational assumptions associated with the DSMC method are the uncoupling of the molecular motion and collisions over small time steps and the division of the flow field into small cells [2, 14]. The time step should be much less than the mean collision time and a typical cell dimension should be much less than the local mean free path [9, 14, 18]. The cell dimension should also be small compared with the distance over which there is a significant change in the flow properties. In practice, the cell size in low Knudsen number flows is set to about one third or one half the cell size [14]. The time step is then set such that a typical molecule moves about one third of the cell dimension at each time step [2]. This satisfies the above requirement for the size of time step in stationary low Knudsen number flows (considered in this paper).

The DSMC method uses the cell system only for the sampling of the macroscopic properties and for the selection of possible collision partners. In addition, the sampled density is used in the procedures for establishing the collision rate [2]. This means that the cell geometry should be chosen to minimize the changes in the macroscopic properties across an individual cell (as in the Code Validation case considered in the Section 3 below). Different implementations of the DSMC method (e.g., alternatives in selecting the collision partners in the cells) were discussed in detail in Refs. 2 and 14. The latest version 3 of DS2G Program [14], that implements the DSMC method, introduces an adaptive transient rectangular background grid to one cell at a time within the collision routine. This yields nearest-neighbor collisions and is efficient with regard to both

computer memory-storage and computation time requirements. The ratio of the time step to the local mean collision time and the ratio of the mean separation between collision partners to the local mean free path should be well under unity over the flowfield area.

The replacement of the extremely large number of real molecules by a significantly smaller number of simulated molecules could result (in a few specific cases) in misinterpretation of some physical phenomena. The serious statistical problem arises when a significant effect in the real gas (e.g., chemical reactions of ionization [18], or quantum effects in rotational-translational relaxation in hypersonic underexpanded jets [8]) is a consequence of the few molecules towards the extremities of the distribution. In general, the statistical scatter decreases as the square root of the sample size and, in order to attain a sufficiently small standard deviation, the programs employ either time averaging for steady flows [9] or ensemble averaging for unsteady flows [14].

3. Computer Code Validation

The two-dimensional DS2G code [14] has been used as a numerical simulation tool in this study. Molecular collisions in argon and nitrogen are modeled using the variable hard sphere molecular model [2]. The gas-surface interactions are assumed to be fully diffusive with full moment and energy accommodation, and the wall temperature is equal to the stagnation temperature.

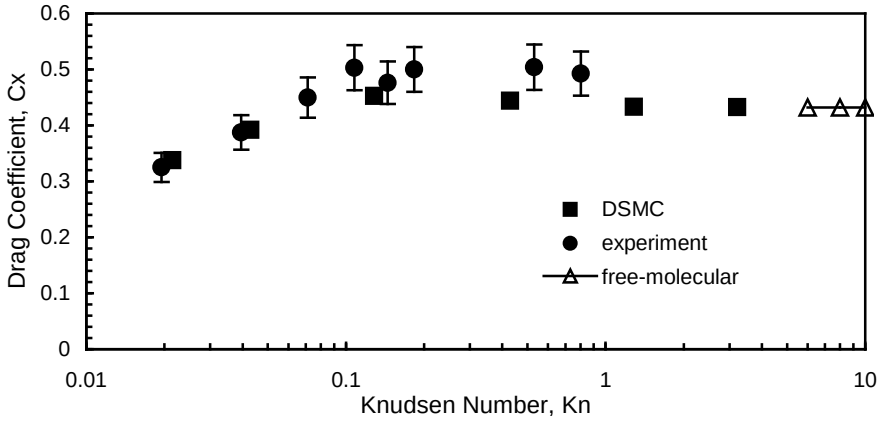

Figure 1. Drag coefficient of a plate vs. Knudsen number $Kn_{\infty,L}$ in air at $M_\infty = 10$ and $\alpha = 0$. Experimental data from Ref. 7.

Code validation was established [9, 10, 28] by comparing numerical results with experimental data [7, 9] related to simple-shape bodies. As an example, the comparison of the DSMC recent numerical results with experimental data [7] in air is shown in Fig. 1 for a wide range of Knudsen numbers from 0.02 to 3.2 and flow parameters: $M_\infty = 10$, $\gamma = 1.4$, and $t_w = 1$. The error of experimental data [7] (see error bars in Fig. 1) was estimated as 8-12% at different flow regimes (see Ref. 7 and the bibliography in Ref. 9). The numerical results correlate well with experimental data at $0.02 < Kn_{\infty,L} < 1$ and approach the free-molecular limit [3] at $Kn_{\infty,L} > 3$.

The methodology from Refs. 2, 9 and 14 has been applied in computations. The mesh size and the number of molecules per cell were varied until independence of the flow profiles and aerodynamic characteristics from these parameters was achieved for each case [10]. Table 1 shows the DSMC results for the drag coefficient of the plate C_x in the airflow at $Kn_{\infty,L} = 0.13$, $M_\infty = 10$, $\gamma = 1.4$, $t_w = 1$, and different computational parameters. The uniform grid has covered the symmetrical flow area 0.024 m × 0.021 m near the plate 0.01 m × 0.001 m. The location of the external boundary with the upstream flow conditions is at 0.01 m from the leading edge of the plate. It has been found that the numerical solutions for C_x are independent of the numerical parameters (see Table 1).

Table 1. Drag coefficient of a single plate in airflow at $Kn_{\infty,L} = 0.13$, $M_\infty = 10$, $\gamma = 1.4$, $t_w = 1$, and different numerical parameters

Number of cells	Number of molecules per cell	Drag coefficient	Time of calculation
12,700	11	0.4524	12 h. 28 min.
12,700	22	0.4523	21 h. 03 min.
49,400	11	0.4525	62 h. 06 min.
203,200	11	0.4526	187 h. 11 min.

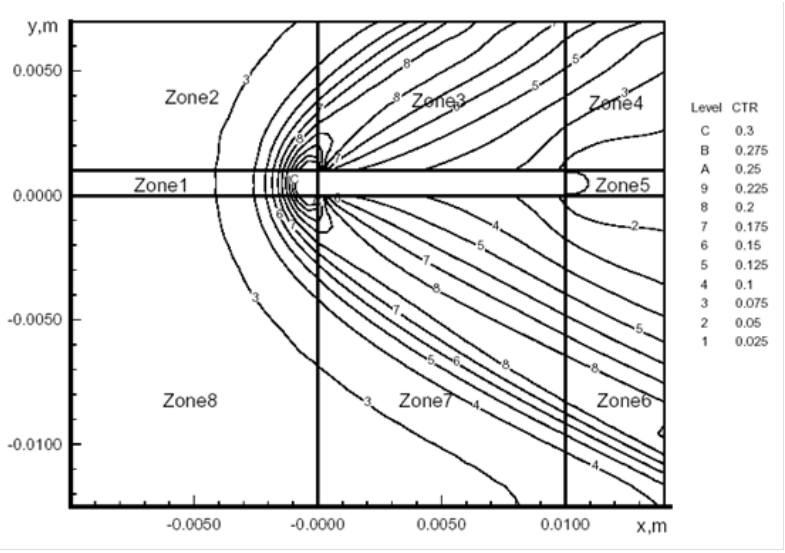

Figure 2. CTR [14] of the time step to the local mean collision time in argon flow about a side-by-side plate at $Kn_{\infty,L} = 0.024$ and $H = 1.25L$.

The similar mesh parameters have been used in the case of two side-by-side plates. As an example, for calculations at $H/L = 1.25$, the total number of cells near a plate (a half-space of the flow segment between side-by-side plates) is 12,700 in eight zones (see Fig. 2), the argon molecules are distributed evenly, and a total number of 139,720 molecules corresponds to an average 11 molecules per cell. The location of the external boundary with the upstream flow conditions varies from $0.75L$ to $1.5L$. Following the recommendations of Refs. 2 and 14, acceptable results are obtained for an average of at least ten molecules per cell in the most critical region of the flow. The error was pronounced when this number falls below five. The cell geometry has been chosen to

minimize the changes in the macroscopic properties (pressure and density) across the individual cell [14]. In all cases the usual criterion [2] for the time step Δt_m has been realized, $1\times10^{-8} \le \Delta t_m \le 1\times10^{-6}$ s. Under these conditions, aerodynamic coefficients and gas-dynamic parameters have become insensitive to the time step. The ratios of the mean separation between collision partners to the local mean free path and the collision time ratio (CTR) [14] of the time step to the local mean collision time have been well under unity over the flowfield (see Fig. 2).

The total number of non-uniform cells [15] near a cylinder (a half-space of the flow segment between side-by-side plates for calculations at $H/R = 3$) is 2100, and 32,200 molecules are distributed evenly (an average 15 molecules per cell). The location of the external boundary varies from 2.5R to 4.5R.

The DS2G program employed time averaging for steady flows [14]. About 200,000 samples have been studied in the considered cases. The computed results have been stored to the TECPLOT® files that have been further analyzed to study whether the DSMC numerical criteria [2] are met. Calculations were carried out on a personal computer with a Pentium® III 850-MHz processor. The computing time of each variant was estimated to be approximately 12 - 60 h.

4. Aerodynamics of a Blunt Plate

The comparison of the DSMC numerical results for a drag coefficient of a plate (thickness $\delta = 0.1L$) with experimental data [7] in air (specific heat ratio $\gamma = 1.4$) is studied for Knudsen numbers $Kn_{\infty,L}$ from 0.02 to 3.2, Mach number $M_\infty = 10$, and temperature factor $t_w = T_w/T_0 = 1$. Numerical results (see Fig. 1) correlate well with experimental data [7] at $0.02 < Kn_{\infty,L} < 1$. The free-molecular limit [3] is approached at $Kn_{\infty,L} > 3$.

The study of the influence of Mach number M_∞ on aerodynamic characteristics of bodies of simple shape was conducted at moderate values of the Knudsen number and at constant values of similarity parameters: $Kn_{\infty,L}$, t_w, and γ. The hypersonic stabilization regime [9] occurs at $M_\infty\theta >> 1$ in the case of streamlining of thin bodies when the angle θ between the generatrix of the body surface and the upstream-flow direction becomes small enough. This regime is realized at smaller values of M_∞, if the angle θ increases.

The results of previous studies [6-8] indicate that the hypersonic flow independency principle [9] is realized in the transition rarefied-flow regime at $K = M_\infty\times\sin\theta > 1$. As was found in experiments [6-8], this principle is not true for thin bodies at small angles of attack in rarefied gas flows under the conditions $K < 1$.

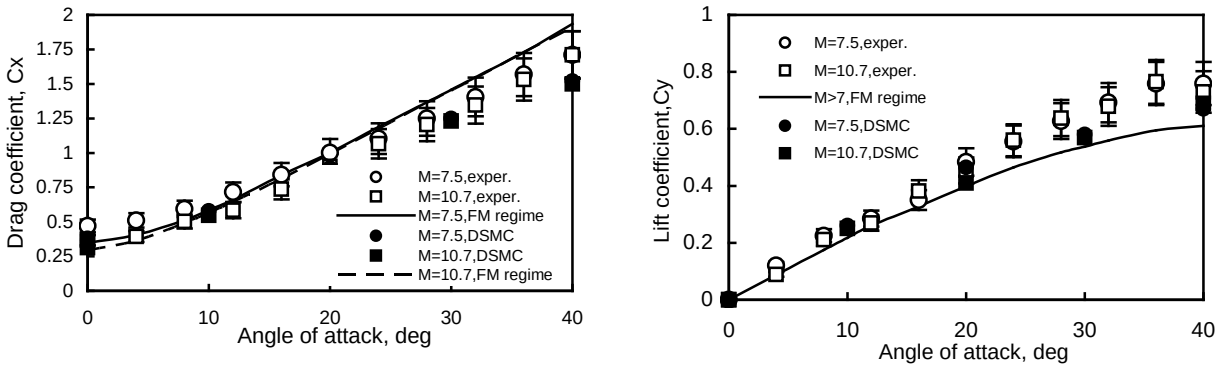

Figure 3. Drag and lift coefficients C_x, C_y for a blunt plate ($\delta = 0.06L$) at $Kn_{\infty,L} = 0.6$ and $M_\infty = 7.5$ (circles) and 10.7 (squares) in helium. Experimental data from Refs. 6-8.

The drag coefficient of a blunt plate having relative thickness $\delta = 0.06L$ becomes sensitive to the magnitude of the freestream Mach number in helium flow (Fig. 3, $M_\infty = 7.5$ and $M_\infty = 10.7$) at small angles of attack $\alpha < 12$ deg. The results calculated by the DSMC technique (filled markers) correlate well with the experimental data [6-8] (empty markers). For the lift coefficient, the free-molecular flow data [3], as well as computational and experimental results presented in Fig. 3, are independent of the Mach number, and the value $C_{y,FM}$ is less by approximately 15% than the value C_y for the transitional flow regime at $\alpha > 16$ deg. This phenomenon was discussed in Refs. 6-9.

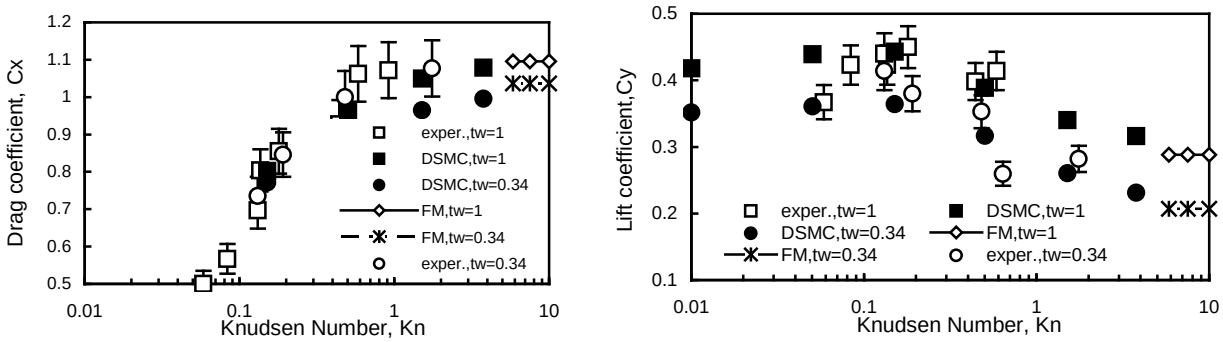

Figure 4. Drag and lift coefficients C_x, C_y for a blunt plate ($\delta = 0.1L$; $\alpha = 20$ deg) in air vs. Knudsen number $Kn_{\infty,L}$ at various temperature factors t_w. Experimental data from [7].

The temperature factor is other important similarity parameter [4-9], which effects pressure at the body surface. Numerical data for a plate ($\delta = 0.1L$) at angle attack $\alpha = 20$ deg and various $Kn_{\infty,L}$ has been studied (see Fig. 4). The lift coefficient, C_y changes non-monotonically from the continuum to the free-molecular flow regime. Maximum values occur in the transition flow regime. The influence of t_w can be estimated as 25% for C_y. The results correlate well with the experimental data [7].

5. Aerodynamics of a Wedge

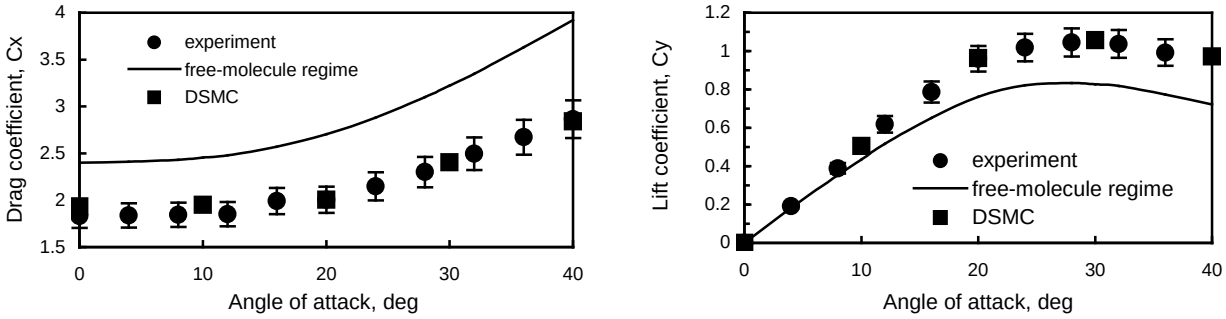

Figure 5. Drag and lift coefficients C_x, C_y for a wedge (θ = 20 deg) in helium flow at $Kn_{\infty,L}$ = 0.3 and M_∞ = 11.8. Experimental data from Refs. 6-9.

The dependence of drag and lift coefficients for a wedge (θ = 20 deg) on the angle of attack has been studied in numerical simulations of helium flow at $Kn_{\infty,L}$ = 0.3, t_w = 1, and the freestream Mach number M_∞ = 11.8. The DSMC results (squares) are shown in Fig. 5 for drag and lift coefficients. The base area of the wedge and its length were taken as the reference area and length. The numerical results correlate well with the experimental data [6-9] (circles), which were obtained in a vacuum wind tunnel at the same flow parameters. In both transitional and free-molecular [3] regimes, the characteristics are not sensitive to changes in upstream flow parameters at $M_\infty > 9$. Another interesting fact is that the lift-drag ratio in the transitional flow regime is larger by 50% than the corresponding parameter in the free-molecular regime [5-9].

6. Aerodynamics of a Disk

In the free-molecular flow regime, the influence of the specific heat ratio γ on the aerodynamic characteristics of bodies depends on the normal component of the momentum of the reflected molecules, which is a function of γ [7-9]. The same phenomenon can be observed at the transitional conditions in the case of the disk at α = 90 deg. The nitrogen-argon pair was the most acceptable one for testing [6-9]. The dependencies of C_x of the disc for Ar (filled triangles) and N_2 (filled squares) are shown in Fig. 6 for a wide range of Knudsen numbers ($Kn_{\infty,D}$). At the same parameters of the upstream flow, numerical data obtained by the DSMC technique for different models of molecules are compared with experimental data [6-8]. This analysis could be applied to the design of a disk ballute [16].

The influence of specific heat ratio on the drag coefficient is more significant for large values of $Kn_{\infty,D} > 1$. In the free molecular regime ($Kn_{\infty,D} > 7$) an increase of C_x is observed as γ increases [3, 9]. This increase is caused by the dependence on γ of the reflected momentum of the molecules at t_w = 1. The degree of this influence has been evaluated as 8% at $Kn_{\infty,D} > 2$. As the number $Kn_{\infty,D}$ decreases, this influence decreases, and at $Kn_{\infty,D} < 0.4$, the drag coefficient of the disk in diatomic gas becomes larger than

that for a monatomic gas. In the continuum flow regime, the dependence of the drag-coefficient on γ difference is insignificant.

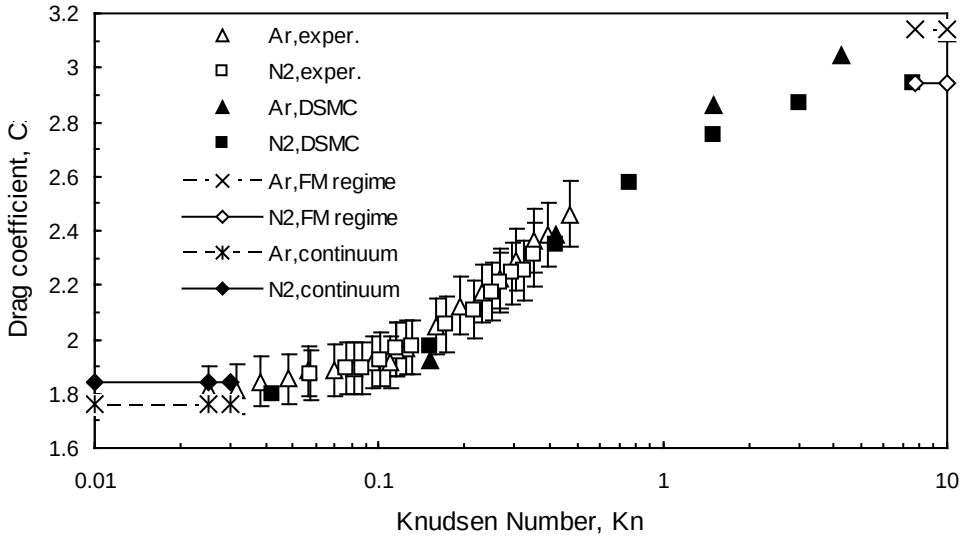

Figure 6. Drag coefficient C_x for a disk (α = 90 deg) vs. Knudsen number $Kn_{\infty,D}$ in argon and nitrogen. Experimental data from Refs. 6-8.

7. Aerodynamics of Two Side-by-Side Plates

The flow pattern over two side-by-side plates is sensitive to the geometrical parameter, H/L, where $2H$ is a distance between the plates. The influence of this parameter on the flow structure was studied for flow of argon at M_∞ = 10, t_w = 1, and $0.024 \le Kn_{\infty,L} \le 1.8$. At $H \le 0.5L$, the flow area between two side-by-side plates becomes subsonic [10]. At $H > 0.5L$, two oblique shock waves interact in the vicinity of the symmetry plane generating the normal shock wave and the Mach reflected waves far behind the bodies [10].

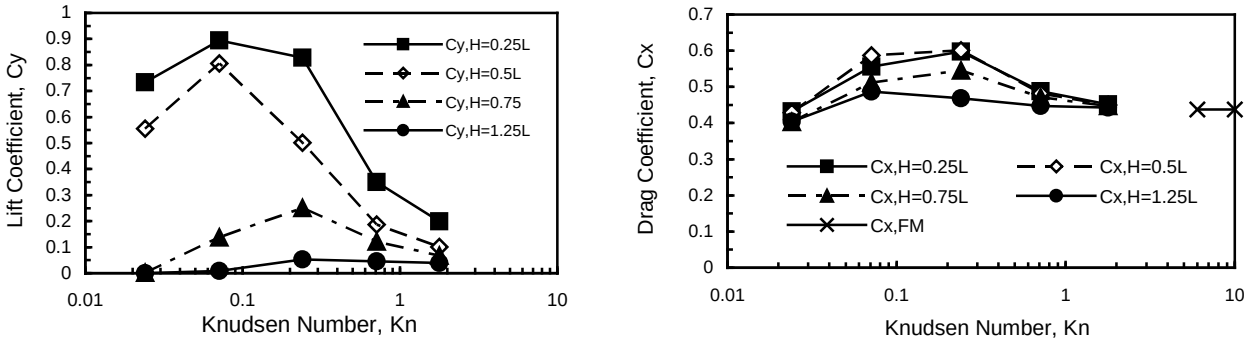

Figure 7. Lift and drag coefficients C_y, C_x of the side-by-side plates in argon vs. Knudsen Number $Kn_{\infty,L}$ at M_∞ = 10.

Numerical results for lift and drag coefficients are shown in Fig. 7. The repulsive lift force becomes significant at $H/L \le 0.75$, with the average lift-drag ratio of 1.6 for plates in the transition regime [10]. The rarefaction effects are responsible for non-monotonic dependency of the lift on the Knudsen number at $1.25 \ge H/L \ge 0.25$. The drag coefficient (Fig. 7) increases with Knudsen number, reaches a maximum, and then decreases to the free-molecular value [3]. The geometrical factor becomes insignificant as to its influence on the drag as both the continuum and free-molecule flow regimes are approached.

8. Aerodynamics of a Torus

Strong influences of the geometrical factor, H/R (ratio of the distance between the axis of symmetry and the torus disk center H, and the torus cross-section radius R) and the Knudsen number, $Kn_{\infty,R}$ on the flow structure near a torus (the shape of shock waves and the stagnation point location), skin friction, pressure distribution, and drag have been found. The influence of these parameters on the flow structure has been studied in argon, nitrogen, and carbon dioxide at $M_\infty = 10$, $2R \le H \le 8R$, and $0.0167 \le Kn_{\infty,R} \le 10$.

At values of the parameter $H/R > 6$, the conical shock waves interact in the vicinity of the flow symmetry axis far beyond the torus throat, creating the Mach disk. The reflected conical wave has a different pattern of the interaction with the supersonic flow behind a torus in continuum and rarefied flow regimes [11]. At $H/R \ge 8$, the flow near a torus is similar to that one about two side-by-side cylinders [15].

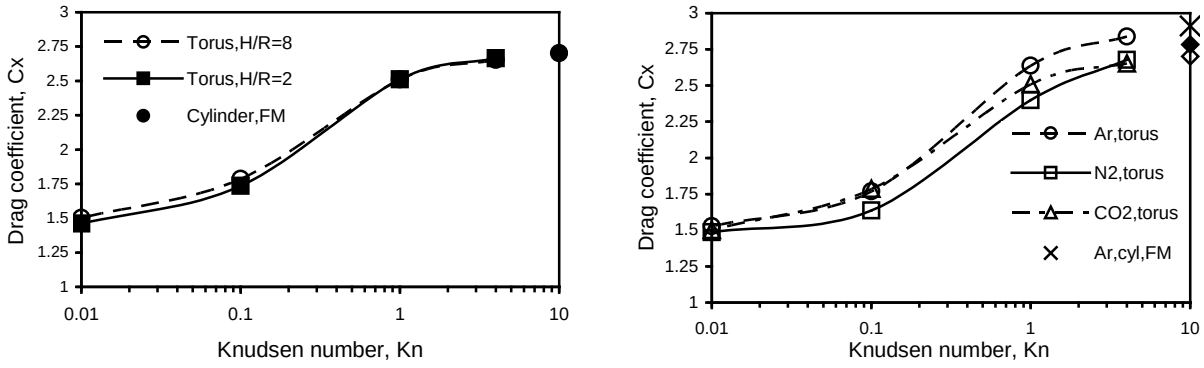

(a) Drag coefficient C_x of a torus in carbon dioxide

(b) Drag coefficient C_x of a torus ($H/R \ge 6$) in Ar, N_2, and CO_2

Figure 8. Drag coefficient C_x of a torus vs. Knudsen number $Kn_{\infty,D}$ in argon, nitrogen, and carbon dioxide at $M_\infty = 10$.

At smaller values of the parameter $H/R \le 4$, the shape of a front shock wave becomes normal, and the subsonic area is restricted by the location of the shock wave and the torus throat [11]. This "chocked-flow" effect plays a fundamental role in the redistribution of pressure and skin friction along the torus surface. The location of the stagnation-point ring (estimated through distributions of pressure and skin-friction coefficients) is moving from the front area to the torus throat after reducing the outer torus radius, H.

Numerical results of the total drag coefficient of a torus are also studied (see Fig. 8). The drag coefficient increases with increasing the Knudsen number. The geometrical factor becomes insignificant on the drag at $H/R \geq 6$ under continuum and free-molecule flow regimes. Heat transfer on toroidal ballutes was studied in Refs. 18, 30-32.

9. Aerodynamics of a Rotating Cylinder

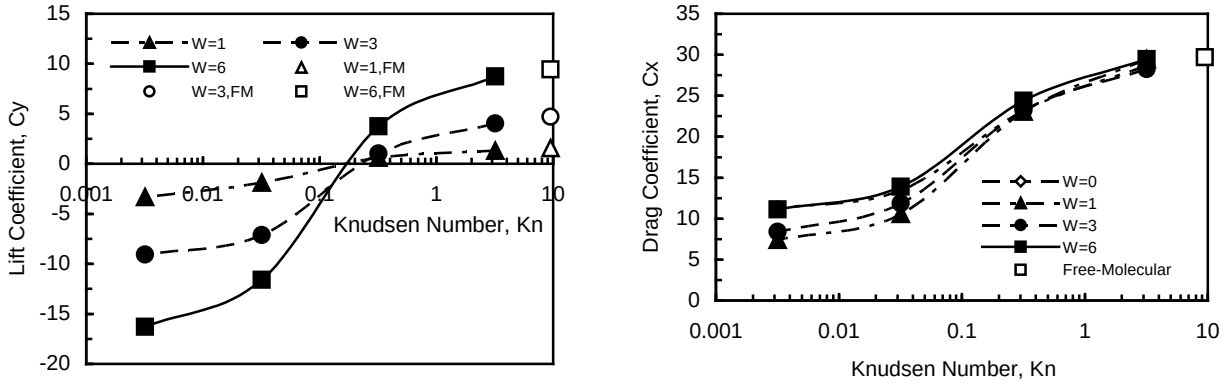

Figure 9. Lift and drag coefficients C_y, C_x of a spinning cylinder vs. Knudsen number $Kn_{\infty,D}$ at $M_\infty = 0.15$ and different spin rates W in argon.

At subsonic flow conditions, the speed ratio $S = M_\infty \cdot (0.5 \cdot \gamma)^{1/2}$ becomes small, and aerodynamic coefficients of a rotating cylinder become sensitive to the ratio magnitude [3, 13, 19]. The transition flow regime has been studied in argon at $M_\infty = 0.15$ and spin ratio $W = \Omega D/2U_\infty = 1$, 3, and 6. The lift and drag coefficients are shown in Fig. 9.

In the transition flow regime ($Kn_{\infty,D} > 0.03$), both the incident and reflected molecules significantly influence the lift [13]. The incident molecules dominate when $Kn_{\infty,D} < 0.1$, and the reflected molecules dominate when $Kn_{\infty,D} > 0.1$. The lift changes sign for the cylinder spinning in counter-clockwise direction. The drag becomes a slow function of the spin rate. In the near-free-molecule flow regime ($Kn_{\infty,D} = 3.18$), the asymmetry of the flow in upper and bottom regions is significant [13]. The flow disturbances are concentrated in the vicinity of the spinning surface. In the near-continuum flow regime ($Kn_{\infty,D} = 0.032$), the circulating zone is much wider. These flow-pattern differences dominate the character of molecule-surface interactions.

At supersonic flow conditions, the speed ratio S becomes large, and the aerodynamic coefficients become less sensitive to its magnitude [13, 19]. In the present study, the transition flow regime has been investigated numerically at $M_\infty = 10$, $\cdot\gamma = 5/3$ (argon gas), and spin ratio $W = 0.03$ and $W = 0.1$.

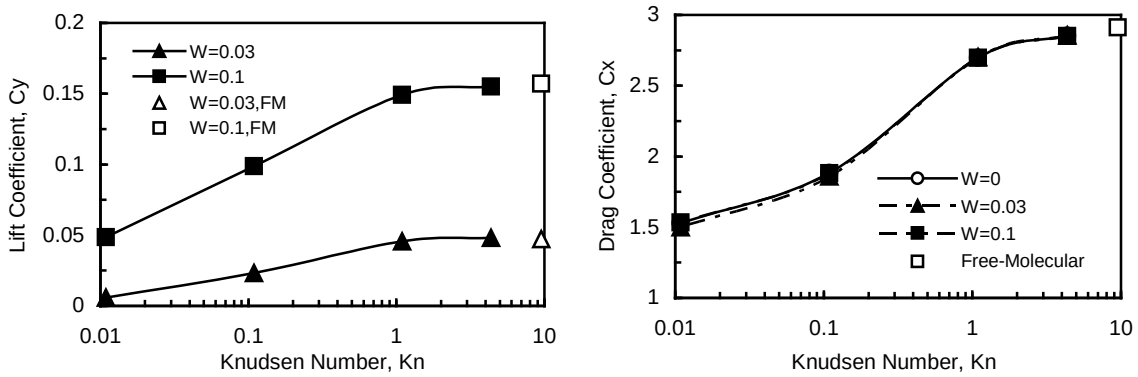

Figure 10. Lift and drag coefficients C_y, C_x of a spinning cylinder vs. Knudsen number $Kn_{\infty,D}$ at $M_\infty = 10$ and different spin rates W in argon.

The lift and drag coefficients are shown in Fig. 10. For the lift coefficient, the influence of reflected molecules is dominant in the transition-flow regime ($Kn_{\infty,D} > 0.03$). The incident-molecule input becomes significant at Knudsen number $Kn_{\infty,D} < 0.1$ [13]. Under the considered flow conditions, the lift coefficient has a positive sign (which is opposite to the sign under the continuum flow regime) for the cylinder spinning in a counter-clockwise direction. The drag is insensitive to the spin rate. The values of C_y and C_x at $Kn_{\infty,D} > 4$ are near the magnitudes of the coefficients for the free-molecule flow [3, 19].

The flow characteristics are different in these cases [13]. For a small spin rate, $W = 0.1$, the zone of circulating flow is located in the vicinity of the surface, and it does not affect the flow zone located far from the surface. The flow pattern becomes asymmetrical. The differences in flow patterns dominate the character of molecule-surface interactions, and they characterize the differences in performance parameters under significantly distinct flow conditions [13]. Similar effects for a spinning sphere were studied in [20, 21].

Concluding Remarks

Students' projects have revealed new information about hypersonic viscous rarefied-gas flows near simple-shape bodies that can be effectively used for investigation and prediction of aerothermodynamic characteristics of hypersonic probes and vehicles during the design of their missions in complex rarefied atmospheric conditions of the Earth, Mars, Venus, and other planets. Fundamental insight into the characteristics and similarity parameters of these flows was obtained. For conditions approaching the hypersonic limit, the Knudsen number $Kn_{\infty,L}$ (or the equivalent Reynolds number Re_0) and temperature factor t_w are the primary similarity parameters. The influence of other parameters (the specific heat ratio γ, viscosity parameter n, and Mach number M_∞) is significant at $M_\infty\theta << 1$ and $Re_0 < 10$. The abnormal increase in the pitching momentum coefficient for the blunt plate and the drag coefficient of the sharp cone at low Reynolds numbers should be verified in future experiments and numerical calculations based on three-dimensional non-uniform flow analysis.

The hypersonic rarefied-gas flows about two side-by-side plates and cylinders in argon have been studied using the direct simulation Monte-Carlo technique. The flow pattern and shock-wave shapes are significantly different for small and large geometric ratios. At a value of the geometrical ratio parameter H/L of 0.5, the disturbances interact in the vicinity of the symmetry plane, creating a normal shock wave and a wide subsonic area, which occupies the whole ‘‘throat” area between the plates. This phenomenon affects the drag, pressure and skin-friction distributions along the plates, and produces significant repulsive lift force. A non-monotonic dependency of lift, drag and lift-drag ratio vs. Knudsen number has been found for different geometric factors. The rarefaction effects on the lift force are significant at all considered values of the geometric factor ($1.25 > H/L > 0.25$), and they are responsible for non-monotonic dependency of the lift force and lift-drag ratio with the maximum value of 1.7.

The similar effects have been found in the case of hypersonic argon flow about two side-by-side cylinders. At the small ratio parameters, $H/R < 1$, the front shock-wave shape becomes normal, a wide subsonic area occupies the whole ‘‘throat” area between the cylinders, and the front stagnation points relocate from the cylinder front zone to the throat area. This phenomenon affects the drag, pressure and skin-friction distributions along the cylinders.

Hypersonic flows about a toroidal balloon and its aerodynamic characteristics have been investigated in nitrogen, argon, dissociating oxygen, and carbon dioxide at $8R > H > 2R$ and the Knudsen number $Kn_{\infty,D}$ from 0.005 to 10. The effect of dissociation on chocking of ducted flows has been studied numerically for a ballute model with varying an aspect area ratio, H/H^*. The present study confirms the Lourel’s hypothesis [32] that the flow of dissociating oxygen is not choked at the ‘‘designed” toroid with a throat radius $H^* = 0.014$ m, but the flow of perfect gas is choked at the similar conditions.

Finally, It has been found that the lift force on a spinning cylinder (“the Magnus effect”) at subsonic upstream conditions has different signs in the free-molecule and continuum regimes. The lift-force sign change occurs in the transition regime at Knudsen number of 0.2.

Acknowledgements

The author would like to express gratitude to Dr. G. A. Bird for the opportunity of using the DS2G computer program, and to Dr. J. N. Moss and Dr. M. S. Ivanov for valuable discussions of the DSMC technique.

References

[1] Gnoffo, P. A., “Computational Aerothermodynamics in Aeroassist Applications,” *J. Spacecraft and Rockets* **40** (3), 305-312 (2003).
[2] Bird, G. A., *Molecular Gas Dynamics and the Direct Simulation of Gas Flows*, 1st ed., Oxford University Press, Oxford, England, UK, 1994, pp. 340-377.
[3] Kogan, M. N., *Rarefied Gas Dynamics*, Plenum Press, New York, 1969, pp. 345-390.

[4] Koppenwallner, G., and Legge, H., “Drag of Bodies in Rarefied Hypersonic Flow” in *Thermophysical Aspects of Re-Entry Flows*, edited by J. N. Moss and C. D. Scott, AIAA, Washington, DC, 1994, pp. 44-59.
[5] Gusev, V. N., Kogan, M. N., and Perepukhov, V. A., "The Similarity and Aerodynamic Measurements in Transitional Regime at Hypersonic Velocities," *Uchenyye Zapiski TsAGI* **1** (1), 24-31 (1970) (in Russian).
[6] Gusev, V. N., Klimova, T. V., and Riabov, V. V., “The Basic Characteristics of the Variation of Aerodynamic Parameters in the Transition Regime at Hypersonic Flow Velocities,” *Uchenyye Zapiski TsAGI*, **7** (3), 47-57 (1976) (in Russian).
[7] Gusev, V. N., Erofeev, A. I., Klimova, T. V., Perepukhov, V. A., Riabov, V. V., and Tolstykh A. I., Theoretical and experimental studies of flow over bodies of simple shape by a hypersonic stream of rarefied gas. *Trudy TsAGI* **1855**, 3-43 (1977) (in Russian).
[8] Riabov, V. V., Aerodynamic applications of underexpanded hypersonic viscous jets. *J. Aircraft* **32** (3), 471-479 (1995).
[9] Riabov, V. V., Comparative analysis of hypersonic rarefied gas flows near simple-shape bodies. *J. Spacecraft and Rockets* **35** (4), 424-433 (1998).
[10] Riabov, V. V., Aerodynamics of two side-by-side plates in hypersonic rarefied-gas flows. *J. Spacecraft and Rockets* **39** (6), 910-916 (2002).
[11] Riabov, V. V., Numerical study of hypersonic rarefied-gas flows about a torus. *J. Spacecraft and Rockets* **36** (2), 293-296 (1999).
[12] Riabov, V. V., Heat transfer on a hypersonic sphere with diffuse rarefied-gas injection. *J. Spacecraft and Rockets* **41** (4), 698-703 (2004).
[13] Riabov, V. V., Aerodynamics of a spinning cylinder in rarefied gas flows. *J. Spacecraft and Rockets* **36** (3), 486-488 (1999).
[14] Bird, G. A., “The DS2G program User’s Guide. Version 3.2,” G. A. B. Consulting Pty, Killara, Australia, 1999, pp. 1-56.
[15] Riabov, V. V., Interference between two side-by-side cylinders in hypersonic rarefied-gas flows. AIAA Paper 2002-3297. Washington, DC: AIAA; 2002, 1-9.
[16] McRonald, A., A Light-Weight Inflatable Hypersonic Drag Device for Planetary Entry. AIAA Paper 99-0422, Association Aeronautique de France Conference, Arcachon, France, March 16-18 1999.
[17] Hall, J., A Review of Ballute Technology for Planetary Aerocapture. Paper IAA-L-1112, 4th IAA Conference on Low Cost Planetary Missions, Laurel, MD, May 2-5 2000.
[18] Moss, J. N., Direct Simulation Monte Carlo Simulations of Ballute Aerothermodynamics under Hypersonic Rarefied Conditions. *J. Spacecraft and Rockets* **44** (2), 289-298 (2007).
[19] Ivanov, S., and Yanshin, A., “Forces and Moments Acting on Bodies Rotating About a Symmetry Axis in a Free Molecular Flow,” *Fluid Dynamics* **15** (3), 449-453 (1980).
[20] Borg, K. I., and Söderholm, L. H., “Orbital Effects of the Magnus Force on a Spinning Spherical Satellite in a Rarefied Atmosphere,” *European J. of Mechanics - B/Fluids* **27** (5), 623-631 (2008).
[21] Volkov, A. N., “Aerodynamic Coefficients of a Spinning Sphere in a Rarefied-Gas Flow,” *Fluid Dynamics* **44** (1), 141-157 (2009).
[22] Yegorov, I. V., Yegorova, M. V., Ivanov, D. V., and Riabov, V. V., “Numerical Study of Hypersonic Viscous Flow about Plates Located Behind a Cylinder,” AIAA Paper 97-2573. Washington, DC: AIAA; 1997, 1-10.
[23] Gnoffo, P. A., and Anderson, B. P., “Computational Analysis of Towed Ballute Interactions,” AIAA Paper 2002-2997. Washington, DC: AIAA; 2002, 1-9.
[24] Riabov, V. V., and Botin, A. V., “Hypersonic hydrogen combustion in the thin viscous shock layer,” *J Thermophys Heat Transfer* 1995; **9**(2): 233-39.

[25] Ferziger, J., and Kaper, H. G., *Mathematical Theory of Transport Processes in Gases*, Amsterdam: North-Holland, 1972, pp. 37-229.
[26] Bird, G. A., "Direct Simulation of the Boltzmann Equation," *Phys Fluids* 1970; **13**(11): 2676-2681.
[27] Riabov, V. V., "Numerical Study of Hypersonic Rarefied-Gas Flows about a Toroidal Ballute." In: Rarefied Gas Dynamics, edited by Ivanov, M.S., and Rebrov, A. K. 25th Intern. Symposium Proceedings. Novosibirsk, Russian Academy of Sciences; 2007, pp. 765-770.
[28] Riabov, V. V., "Numerical Study of Interference between Simple-Shape Bodies in Hypersonic Flows," *Computers and Structures*, 2009; **87**: 651-663.
[29] Gorelov, S. L, and Erofeev, A. I., "Qualitative Features of a Rarefied Gas Flow about Simple Shape Bodies." In: Rarefied Gas Dynamics, edited by Belotserkovskii, O. M, Kogan, M. N, Kutateladze, S. S, and Rebrov, A. K. 13th Intern. Symposium Proceedings, Vol. 1. New York, NY: Plenum Press; 1985, pp. 515-21.
[30] McIntyre, T. J., Lourel, I., Eichmann, T. N., Morgan, R. G., Jacobs, P. A., and Bishop, A. I., "Experimental Expansion Tube Study of the Flow over a Toroidal Ballute," *J Spacecraft and Rockets* 2004; **41**(5):716-725.
[31] Lourel, I., Eichmann, T. N., Isbister, S., McIntyre, T. J., Houwing, A. F. P., and Morgan, R. G., "Experimental and Numerical Studies of Flows about a Toroidal Ballute." Proceedings of the 23rd International Symposium on Shock Waves, Paper 5038. Fort Worth, TX, July 22-27, 2001; pp. 1-7.
[32] Lourel, I., and Morgan, R. G., "The Effect of Dissociation on Chocking of Ducted Flows." AIAA Paper 2002-2894. Washington, DC: AIAA; 2002, 1-11.